One- and two-dimensional gap solitons in spin-orbit-coupled systems with Zeeman splitting

Hidetsugu Sakaguchi and Boris A. Malomed

Phys. Rev. A **97**, 013607 — Published 10 January 2018

DOI: 10.1103/PhysRevA.97.013607

One- and two-dimensional gap solitons in spin-orbit-coupled systems with Zeeman splitting

Hidetsugu Sakaguchi[1] and Boris A. Malomed[2,3]
[1] *Department of Applied Science for Electronics and Materials, Interdisciplinary Graduate School of Engineering Sciences, Kyushu University, Kasuga, Fukuoka 816-8580, Japan*
[2] *Department of Physical Electronics, School of Electrical Engineering, Faculty of Engineering, and Center for Light-Matter Interaction, Tel Aviv University, Tel Aviv 69978, Israel*
[3] *ITMO University, St. Petersburg 197101, Russia*

We elaborate a mechanism for the formation of stable solitons of the semi-vortex type (with vorticities 0 and 1 in their two components), populating a finite bandgap in the spectrum of the spin-orbit-coupled binary Bose-Einstein condensate with the Zeeman splitting, in the two-dimensional free space, under conditions which make the kinetic-energy terms in the respective coupled Gross-Pitaevskii equations negligible. Unlike a recent work which used long-range dipole-dipole interactions to construct stable gap solitons in a similar setting, we here demonstrate that stable solitons are supported by generic local interactions of both attractive and repulsive signs, provided that the relative strength of the cross/self interaction in the two-component system does not exceed a critical value ≈ 0.77. A boundary between stable and unstable fundamental 2D gap solitons is precisely predicted by the Vakhitov-Kolokolov criterion, while all excited states of the 2D solitons, with vorticities $(m, 1+m)$ in the two components, $m = 1, 2, ...$, are unstable. The analysis of the one-dimensional (1D) reduction of the system produces an exact analytical solution for the family of gap solitons which populate the entire bandgap, the family being fully stable. Motion of the 1D solitons in the trapping potential is considered too, showing that their effective mass is positive or negative if the cubic nonlinearity is attractive or repulsive, respectively.

I. INTRODUCTION

The realization of the settings which emulate the spin-orbit (SO) coupling in ultracold atomic gases [1–4] has opened up a vast research area in studies of matter waves. In particular, the interplay of the linear SO coupling with intrinsic nonlinearity of Bose-Einstein condensates (BECs) suggests many possibilities for the creation of vortices [5], monopoles [6], skyrmions [7]. Solitons have been predicted too, in both one-dimensional [8] (including dark solitons in rinng-shaped condensates [9]) and two-dimensional (2D) [11] geometries. A remarkable fact is that the SO coupling makes it possible to stabilize 2D [10, 13] and three-dimensional (3D) [12] solitons created by the cubic attractive nonlinearity in the free space, while, in the usual 2D and 3D models, solitons supported by cubic terms are always unstable because of the presence of the critical (2D) and supercritical (3D) collapse [14–16]. Depending on the relative strength of the self- and cross-attractive nonlinear interactions in the spinor (two-component) SO-coupled BEC, the stable 2D and 3D solitons are *semi-vortices* (alias *half-vortices* [17, 18]), with one vortical and one zero-vorticity components, or *mixed modes*, which combine vortical and zero-vorticity terms in both components [10, 12, 13].

Recently, a new approach to the creation of stable 2D solitons in the free-space BEC was proposed in Ref. [19]. If the usual kinetic-energy terms may be neglected in the respective system of Gross-Pitaevskii equation (GPEs), the combination of the SO-coupling of the Rashba type [20] and Zeeman splitting (which is a common ingredient of the SO-coupling settings [21]) replace the usual spectrum, determined by the atomic mass, by one with a finite bandgap, which may be populated by families of gap solitons, under the action of the attractive or repulsive nonlinearity. The creation of gap solitons was first predicted [22] and demonstrated experimentally [23], in an effectively 1D geometry, in optical Bragg gratings, and later in exciton-polariton condensates loaded in photonic lattices [24]. 1D gap solitons were also predicted [25] and experimentally created [26] in the single-component BEC trapped in an optical-lattice potential.

Getting back to the setting for the creation of 2D gap solitons proposed in Ref. [19], it is relevant to note that, as demonstrated in that work, if the model of the SO-coupled spinor BEC is effectively reduced from 3D to 2D by sufficiently tight trapping potential acting in the direction perpendicular to the 2D plane, the kinetic-energy terms indeed turn out to be negligible in comparison with the SO-coupling ones. Thus, the respective 2D system with the finite bandgap in the spectrum is quite a generic one. It is relevant to mention that a possibility to neglect the kinetic-energy terms in the SO-coupled BEC was demonstrated too in another setting, based on a lattice potential which creates a *flatband* in the respective spectrum [27].

The two-component BECs which implement the SO coupling are usually realized as mixtures of two different hyperfine atomic states. Accordingly, the natural strengths of the self- and cross-interaction in this binary systems may be close [28]. Therefore, equal strengths of the contact self- and cross-attraction were adopted in Ref. [19].

The analysis has demonstrated that such a model fails to create stable 2D gap solitons. For this reason, long-range interactions were considered instead of the local nonlinearity, assuming that the atoms in both states carry a permanent magnetic dipole moment. This assumption is upheld by the prediction of the realization of the SO coupling in a two-component dipolar BEC [29]. Furthermore, various effects which are possible due to the interplay of the SO coupling and dipole-dipole interactions, were elaborated in a number of works [30]. It has been demonstrated in Ref. [19] that the dipole-dipole interactions, both isotropic repulsive ones, in case the dipole moments are polarized perpendicular to the system's plane, and anisotropic interactions for the in-plane orientation of the moments [31], readily create families of chiefly stable solitons populating the entire system's bandgap. Moreover, the families extend as (partly stable) *embedded solitons* [32] into a band across the gap's top edge.

The possibility of the creation of *stable* 2D gap solitons, and their 1D counterparts, making use of solely *local* self- and cross-interactions in the binary BEC is a challenging issue which is the subject of the present work. An essential finding is that a subfamily of 2D solitons of the semi-vortex type is stable, in the top part of the bandgap, provided that the ratio of the strengths of the cross- and self-interaction in the binary system takes values $\gamma < \gamma_{\max} \approx 0.77$, see Eq. (34) below. This finding explains the absence of stable 2D gap solitons in Ref. [19], which only addressed the local nonlinearity with $\gamma = 1$. It is relevant to mention that γ may be altered, in broad limits, by means of the Feshbach-resonance technique, applying dc magnetic field to the binary BEC [33] (the long-range dipole-dipole interactions can also be adjusted by means of experimentally available methods [34]). We find in this work that a boundary between stable and unstable subfamilies of 2D semi-vortex solitons inside the bandgap is precisely predicted by the well-known Vakhitov-Kolokolov criterion [35, 36]. At the above-mentioned critical value of the relative strength of the cross-interaction, $\gamma = \gamma_{\max} \approx 0.77$, the boundary merges into the top edge of the finite bandgap. It is also relevant to stress that stable bright gap solitons can be supported equally well by the contact interactions of either sign, attractive or negative.

The rest of the paper is organized as follows. The model, based on coupled 2D GPEs and their 1D reduction, is formulated in Section II. The analysis starts with the consideration of the reduced 1D system in Section III. A full family of 1D gap solitons is found in an exact analytical form, and is demonstrated to be completely stable. In addition to finding the solitons in the free space, in the same section we consider motion of the 1D gap solitons in an external trapping potential, concluding that the effective soliton's mass is positive and negative if the contact nonlinearity is, respectively, attractive or repulsive (in the latter case, the trapping potential acts as an expulsive one). The above-mentioned findings for 2D gap solitons of the semi-vortex type are summarized in Section IV. The paper is concluded by Section V.

II. THE GROSS-PITAEVSKII EQUATIONS

The starting point is a scaled system of GPEs (with the atomic mass and $\hbar$ replaced by unity) for two components of the spinor wave function, $\Phi_{\pm}(X, Y, t)$ in the 2D space [8]-[11]:

$$\begin{aligned} i\frac{\partial \Phi_+}{\partial t} &= -\frac{1}{2}\nabla^2\Phi_+ + \lambda\left(\frac{\partial \Phi_-}{\partial X} - i\frac{\partial \Phi_-}{\partial Y}\right)\Phi_- + \Omega\Phi_+ \\ &\quad - \left(g|\Phi_+|^2 + \gamma|\Phi_-|^2\right)\Phi_+, \\ i\frac{\partial \Phi_-}{\partial t} &= -\frac{1}{2}\nabla^2\Phi_- - \lambda\left(\frac{\partial \Phi_+}{\partial X} + i\frac{\partial \Phi_+}{\partial Y}\right)\Phi_+ - \Omega\Phi_- \\ &\quad - \left(\gamma|\Phi_+|^2 + g|\Phi_-|^2\right)\Phi_-, \end{aligned} \tag{1}$$

where g and γ are coefficients of the self- and cross-interactions of the components (their positive and negative values correspond, respectively, to attractive and repulsive interactions), while λ and $\Omega > 0$ represent the strength of the SO coupling and Zeeman splitting (the latter effect may be replaced by the Stark - Lo Surdo splitting induced by dc electric field). These equations are derived from the full 3D GPE system, assuming that the system is subject to tight confinement in the transverse direction, with a trapping size $a_\perp$. This derivation implies, as usual, that the 2D model is relevant for modes (solitons) with lateral sizes $l \gg a_\perp$.

The SO-coupling effect in experimentally available settings is relevant if it is strong enough, namely, $\lambda \gtrsim 1/a_\perp$, in the present notation [18]. In the combination with condition $l \gg a_\perp$, this inequality implies

$$l\lambda \gg 1. \tag{2}$$

Then, the ratio of the kinetic-energy and SO-coupling terms in Eq. (1), obviously estimated as $(l\lambda)^{-1}$, clearly implies that the kinetic energy is negligible, which makes it possible to reduce Eq. (1) to the simplified form, without the

second derivatives and with $(X,Y)/\lambda \equiv (x,y)$, cf. Ref. [19]:

$$
\begin{aligned}
i\frac{\partial \Phi_+}{\partial t} &= \left(\frac{\partial \Phi_-}{\partial x} - i\frac{\partial \Phi_-}{\partial y}\right) - (g|\Phi_+|^2 + \gamma|\Phi_-|^2)\Phi_+ + \Omega\Phi_+, \\
i\frac{\partial \Phi_-}{\partial t} &= -\left(\frac{\partial \Phi_+}{\partial x} + i\frac{\partial \Phi_+}{\partial y}\right) - (\gamma|\Phi_+|^2 + g|\Phi_-|^2)\Phi_- - \Omega\Phi_-.
\end{aligned}
\tag{3}
$$

This is the basic model considered in the present work. If the nonlinear and Zeeman terms are absent, Eq. (3) is tantamount to the 2D equation for Weyl fermions, which, in particular, finds its realization as a model of graphene [38]. Equation (3) is also similar to 2D nonlinear Dirac equations which were recently considered in different contexts [39–41], although in the latter works the cubic nonlinearity is not sign-definite, unlike Eq. (3).

The 1D reduction of the system (when coordinate y is absent) amounts to the following equations:

$$
\begin{aligned}
i\frac{\partial \Phi_+}{\partial t} &= \frac{\partial \Phi_-}{\partial x} - (g|\Phi_+|^2 + \gamma|\Phi_-|^2)\Phi_+ + \Omega\Phi_+, \\
i\frac{\partial \Phi_-}{\partial t} &= -\frac{\partial \Phi_+}{\partial x} - (g|\phi_-|^2 + \gamma|\Phi_+|^2)\Phi_- - \Omega\Phi_-.
\end{aligned}
\tag{4}
$$

Strictly speaking, the reduction of the effective dimension from 2 to 1, as well as from 3 to 2, or directly from 3 to 1, gives rise to additional higher-order nonlinear terms; in particular, small effective quintic terms are generated by the cubic ones in the underlying 3D GPE [42, 43], or in a system of coupled GPEs [44]. In the present context, such additional terms are insignificant, as the simple cubic one readily give rise to stable gap solitons, as shown below.

The linearization of Eqs. (3) and (4) for plane-wave solutions, $\Phi_\pm \sim e^{ik_x x + ik_y y - i\mu t}$ gives rise to the dispersion relation,

$$
\mu = \pm\sqrt{\Omega^2 + k_x^2 + k_y^2},
\tag{5}
$$

and its 1D reduction (corresponding to $k_y = 0$), which contains an obvious gap, provided that Ω^2 is different from zero [19]. As shown below, the bandgap produced by this spectrum,

$$
\mu^2 \leq \mu_{\max}^2 = \Omega^2,
\tag{6}
$$

is completely populated by gap solitons, in 1D and 2D systems alike.

Before proceeding to the construction of the 1D and 2D gap solitons, it makes sense to briefly discuss what may happen to them under the action of small kinetic-energy terms dropped while deriving Eq. (3) from the full system based on Eq. (1). In terms of the notation which keeps the SO-coupling strength, λ, as an explicit parameter, the change of spectrum (5), caused by the presence of the second derivatives in the full system, eventually closes the bandgap, at large values of wavenumbers $k \sim \lambda$. In the course of extremely long evolution, this will eventually lead to rearrangement of the gap solitons into regular ones, through tunneling across the barrier separating the (quasi-) gap and the range of $k \sim \lambda$. A straightforward estimate demonstrates that, for generic solitons of width l, the tunneling time is exponentially large with respect to parameter $l\lambda$, see Eq. (2). This estimate implies that the rearrangement time is many order of magnitude larger than any realistic experimental time, hence the gap solitons are completely robust objects, if Eq. (3) predict them as stable solutions.

While the present work is chiefly focused on the consideration of quiescent solitons, it makes sense to briefly consider a possibility to generate moving ones too. This is a nontrivial issue, as Eqs. (3) and (4). although written in the free space, do not feature any apparent invariance, such as Galilean or Lorentzian, which would allow one to automatically generate moving solutions from quiescent ones. For this purpose, it is appropriate to introduce moving coordinates, $\tilde{x} \equiv x - c_x t, \tilde{y} \equiv y - c_y t$, where (c_x, c_y) is the 2D velocity vector, and rewrite Eq. (3) in the moving reference frame (cf. a similar approach developed in Ref. [10]):

$$
\begin{aligned}
&i\frac{\partial \Phi_+}{\partial t} - i\left(c_x\frac{\partial \Phi_+}{\partial \tilde{x}} + c_y\frac{\partial \Phi_+}{\partial \tilde{y}}\right) \\
&= \left(\frac{\partial \Phi_-}{\partial \tilde{x}} - i\frac{\partial \Phi_-}{\partial \tilde{y}}\right) - (g|\Phi_+|^2 + \gamma|\Phi_-|^2)\Phi_+ + \Omega\Phi_+, \\
&i\frac{\partial \Phi_-}{\partial t} - i\left(c_x\frac{\partial \Phi_-}{\partial \tilde{x}} + c_y\frac{\partial \Phi_-}{\partial \tilde{y}}\right) \\
&= -\left(\frac{\partial \Phi_+}{\partial \tilde{x}} + i\frac{\partial \Phi_+}{\partial \tilde{y}}\right) - (\gamma|\Phi_+|^2 + g|\Phi_-|^2)\Phi_- - \Omega\Phi_-.
\end{aligned}
\tag{7}
$$

The linearization of Eq. (7) gives rise to the following dispersion relation, cf. Eq. (5):

$$\mu = (c_x k_{\tilde{x}} + c_y k_{\tilde{y}}) \pm \sqrt{\Omega^2 + k_{\tilde{x}}^2 + k_{\tilde{y}}^2}. \tag{8}$$

Simple analysis of Eq. (8) demonstrates that this spectrum contains a reduced bandgap, provided that $c^2 \equiv c_x^2 + c_y^2 < 1$, with width

$$\mu^2 \leq \tilde{\mu}_{\max}^2 = \sqrt{1-c^2}\Omega^2, \tag{9}$$

cf. Eq. (5). Edges of the reduced bandgap (9) correspond to wavenumbers

$$(k_{\tilde{x}}, k_{\tilde{y}}) = \mp (c_x, c_y) / \sqrt{1-c^2}. \tag{10}$$

III. THE ONE-DIMENSIONAL SYSTEM

A. Gap solitons in the free space

We start the analysis with the 1D system, looking for stationary states with chemical potential μ as $\Phi_\pm = e^{-i\mu t}\phi_\pm(x)$. The substitution of this in Eq. (4) leads to equations for real wave function $\phi_\pm(x)$:

$$\begin{aligned} \mu\phi_+ - \phi_-' - \Omega\phi_+ + (g\phi_+^2 + \gamma\phi_-^2)\phi_+ &= 0, \\ \mu\phi_- + \phi_+' + \Omega\phi_- + (g\phi_-^2 + \gamma\phi_+^2)\phi_- &= 0, \end{aligned} \tag{11}$$

with the prime standing for d/dx. Equations (11) are similar to (but different from) the system considered in Ref. [45], which was derived as a model of a skewed dual-core optical waveguide. The exact solution for 1D gap solitons obtained in Ref. [45] suggests a possibility to seek for exact solutions to Eq. (11). To this end, we note that evolution of ϕ_+ and ϕ_- along x in the framework of Eq. (11) conserves the corresponding Hamiltonian,

$$H = -\frac{\mu}{2}\left(\phi_+^2 + \phi_-^2\right) + \frac{\Omega}{2}\left(\phi_+^2 - \phi_-^2\right) - \frac{g}{4}\left(\phi_+^2 + \phi_-^2\right)^2 + \frac{g-\gamma}{2}\phi_+^2\phi_-^2. \tag{12}$$

Then, looking for solutions in the polar form,

$$\phi_+(x) = A(x)\cos\left(\alpha(x)\right), \ \phi_-(x) = A(x)\sin\left(\alpha(x)\right), \tag{13}$$

and taking into account that solitons solutions, vanishing at $x \to \pm\infty$, correspond to $H = 0$, one can use Eq. (12) to eliminate A^2 in favor of α:

$$A^2 = 4\frac{-\mu + \Omega\cos(2\alpha)}{2g - (g-\gamma)\sin^2(2\alpha)}. \tag{14}$$

Then, the substitution of expressions (13) and (14) in Eq. (11) leads to an equation for $\alpha(x)$,

$$\alpha' = -\mu + \Omega\cos(2\alpha), \tag{15}$$

whose solution is easily found:

$$\alpha = \arctan\left[\frac{\Omega-\mu}{\sqrt{\Omega^2-\mu^2}}\tanh(\sqrt{\Omega^2-\mu^2}x)\right]. \tag{16}$$

Note that, unlike the 2D system considered in the next section, which gives rise to both fundamental gap solitons of the semi-vortex type and their excited states (higher-order solitary vortices), the simple 1D equation (15) does not produce higher-order solitons.

The solution based on Eqs. (13)-(14) and (16) yields the family of 1D gap soliton with the chemical potential taking values in bandgap (6). Here and in the next subsection, we consider the gap solitons under the action of the dominant attractive interactions, which means $g > 0$ and $\gamma > -g$ (in particular, the case of $-g < \gamma < 0$ corresponds to the competition of the self-attraction and weaker cross-repulsion).

At the top edge of the bandgap, $\mu = +\Omega$, solution (16) degenerates into $\alpha \equiv 0$. Close to this edge, i.e., at $0 < \Omega^2 - \mu^2 \ll \Omega^2$, the solution takes the form of

$$\tan \alpha_{\mu\to\Omega} \approx \sqrt{\frac{\Omega-\mu}{2\Omega}} \tanh\left(\sqrt{2\Omega\,(\Omega-\mu)}x\right),$$
$$(\phi_+)_{\mu\to\Omega} \approx \frac{\sqrt{2\Omega\,(\Omega-\mu)}}{\cosh\left(\sqrt{2\Omega\,(\Omega-\mu)}x\right)},$$
$$(\phi_-)_{\mu\to\Omega} \approx (\Omega-\mu)\,\frac{\sinh\left(\sqrt{2\Omega\,(\Omega-\mu)}x\right)}{\cosh^2\left(\sqrt{2\Omega\,(\Omega-\mu)}x\right)}, \tag{17}$$

which, in this approximation, does not depend on γ. The norm of the limit-form gap soliton (17),

$$N = \int_{-\infty}^{+\infty} \left[\phi_+^2(x) + \phi_-^2(x)\right] dx, \tag{18}$$

vanishes as $N_{\mu\to\Omega} \approx 2\sqrt{2\Omega\,(\Omega-\mu)}$. At the bottom edge of the bandgap, $\mu = -\Omega$, the solution remains nontrivial, being weakly localized, with $A^2(x) \sim x^{-2}$ at $x \to \pm\infty$, rather than the exponentially localized gap solitons found at $\mu^2 < \Omega^2$:

$$\alpha_{\mu=-\Omega} = \arctan(2\Omega x), \tag{19}$$
$$A^2_{\mu=-\Omega}(x) = 4\Omega \frac{1+4\Omega^2x^2}{g+8\gamma\Omega^2x^2+16g\Omega^4x^4}. \tag{20}$$

While the entire family of the 1D gap solitons is found in the exact form, as given by Eqs. (13)-(14) and (16)-(20), their stability should be studied by means of numerical methods. We used systematic simulations of perturbed evolution of the gap solitons to identify their stability. Nevertheless, a necessary stability condition for the gap-soliton family can be verified in a quasi-analytical form, if the soliton's norm, defined as per Eq. (18), is found as a function of μ [in fact, we consider inverse dependences, $\mu(N)$]. Then, the necessary stability condition for solitons supported by a dominant attractive nonlinearity is provided by the well-known Vakhitov-Kolokolov (VK) criterion, $d\mu/dN < 0$ [35, 36]. It guarantees the absence of imaginary eigenfrequencies in the spectrum of small perturbations around the stationary soliton, which would give rise to an exponentially growing instability; however, the VK criterion cannot detect complex eigenfrequencies, that may generate an oscillatory instability.

While an analytical expression for the norm of the generic gap-soliton solution, which corresponds to Eqs. (13)-(14) and (16), is too cumbersome to display it, the norm of the bandgap-edge soliton, given by Eqs. (19) and (20), can be presented in an explicit form:

$$N(\mu=-1) = \pi\left[\left(1-\sqrt{\frac{\gamma-1}{\gamma+1}}\right)\sqrt{\gamma+\sqrt{\gamma^2-1}}\right.$$
$$\left.+\left(1+\sqrt{\frac{\gamma-1}{\gamma+1}}\right)\sqrt{\gamma-\sqrt{\gamma^2-1}}\right]. \tag{21}$$

Here, to make the expression more compact, it is implied that $g = \Omega = 1$ is fixed by means of scaling, and the expression is written for $\gamma \geq 1$. It is valid too for $\gamma < 1$, as the analytical continuation, which remains real and positive. Note that Eq. (21) amounts to $N \approx 2\pi\sqrt{2/\gamma}$ at $\gamma \to \infty$.

A typical example of a stable gap soliton is shown in Fig. 1(a) for $\Omega = 1$, $\mu = 0.2$, $g = 1$ and $\gamma = 0$. Families of the gap solitons, which entirely fill the bandgap, are represented by the above-mentioned dependences, $\mu(N)$, in Fig. 1(b) for the same values $\Omega = 1$, $g = 1$, and a set of different values of the cross-interaction coefficient, $\gamma = -0.95, -0.5, 0, 1$, and 4. As mentioned above, $\gamma < 0$ implies that the cross-interaction in Eq. (4) is repulsive, while fixed $g = 1$ accounts for the self-attraction of each component of the spinor wave function. It is worthy to note that the VK criterion holds for all families of the 1D gap solitons at all values of μ. In agreement with this fact, systematic simulations demonstrate that the 1D gap solitons are completely stable. In particular, Fig. 1(c) illustrates the stable evolution of a weakly localized bandgap-edge soliton, whose norm is given by Eq. (21).

Lastly, beneath the bandgap, i.e., at $\mu < -\Omega$, exact solutions to Eq. (15) can be found too, in a spatially periodic form:

$$\alpha = -\arctan\left(\sqrt{\frac{\mu-\Omega}{\mu+\Omega}}\tan\left(\sqrt{\mu^2-\Omega^2}x\right)\right) \tag{22}$$

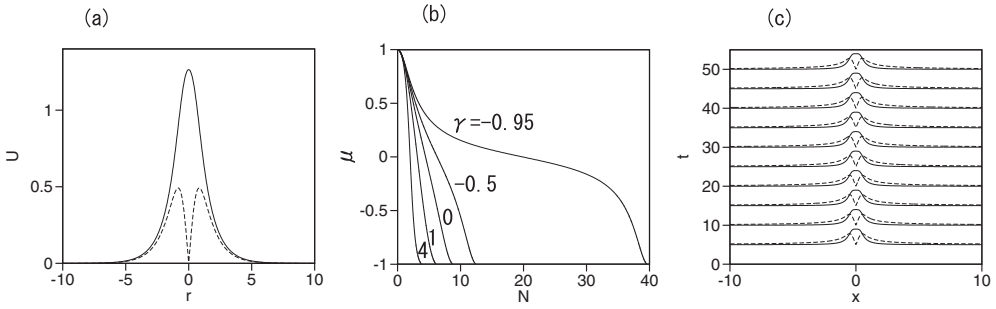

FIG. 1: (a) An exact 1D gap-soliton solution, given by Eqs. (13)-(14) and (16), for $\Omega = g = 1$, $\gamma = 0$, and $\mu = 0.2$. (b) Dependences $\mu(N)$ (the total norm vs. the chemical potential) for the exact gap-soliton families, for $\Omega = g = 1$ and $\gamma = -0.95$, -0.5, 0, 1, and 4. (c) The stable evolution of components $|\Phi_+|$ and $|\Phi_-|$ of the bandgap-edge soliton, given by Eqs. (19) and (20), for $\mu = -1$ at $\Omega = 1$, $g = 1$, and $\gamma = 0$. Plot (c) is produced by simulations of Eq. (4).

[at $\mu > \Omega$, i.e., above the bandgap, solution (22) is irrelevant, as its substitution in Eq. (14) yields $A^2 < 0$]. However, unlike the solitons, these periodic patterns are unstable in direct simulations (not shown here in detail).

B. Dynamics of 1D gap solitons in the trapping potential

Real experiments with BEC are always performed in the presence of trapping, which is usually represented by the harmonic-oscillator potential, $U(x) = (1/2)kx^2$ with $k > 0$. The accordingly modified 1D system of GPEs (4) is

$$\begin{aligned} i\frac{\partial \Phi_+}{\partial t} &= \frac{\partial \Phi_-}{\partial x} - (g|\Phi_+|^2 + \gamma|\Phi_-|^2)\Phi_+ + \frac{1}{2}kx^2\Phi_+ + \Omega\Phi_+, \\ i\frac{\partial \Phi_-}{\partial t} &= -\frac{\partial \Phi_+}{\partial x} - (g|\Phi_-|^2 + \gamma|\Phi_+|^2)\Phi_- + \frac{1}{2}kx^2\Phi_- - \Omega\Phi_-. \end{aligned} \tag{23}$$

It is natural to expect that gap solitons may perform stable shuttle motion in the trapping potential [46] (then, the soliton's zero mode, corresponding to the translational invariance in the free space, turns into a Goldstone mode of small oscillations at the bottom of the potential well, see, e.g., Ref. [37]). This expectation is confirmed by simulations of Eq. (23). In particular, Fig. 2(a) displays the time evolution of $|\Phi_+|$ and $|\Phi_-|$ of a gap soliton which periodically moves in the trap with strength $k = 0.0025$, and Fig. 2(b) shows the evolution of its center-of-mass coordinate,

$$X(t) = \frac{\int_{-\infty}^{+\infty}(|\Phi_+|^2 + |\Phi_-|^2)xdx}{\int_{-\infty}^{+\infty}(|\Phi_+|^2 + |\Phi_-|^2)dx}, \tag{24}$$

initiated by initially placing the gap soliton at $X(t = 0) = -5$. Accordingly, the central coordinate exhibits a sinusoidal motion, $X = -5\cos(\omega t)$ with frequency $\omega = 0.0432$. This result makes it possible to calculate an effective mass of the gap soliton according to the elementary law of harmonic oscillations,

$$m_{\rm eff} = k/\omega^2 \approx 1.34. \tag{25}$$

C. Gap solitons under the action of the repulsive interactions

Repulsive nonlinearity can support gap solitons in the free space as well as it is done by the self-attraction [26, 46, 48]. Indeed, starting from Eqs. (3) or (4) with $g < 0$, one can invert the sign of the nonlinearity coefficients, g and γ, by the substitution of $\Phi_+ \to \Phi_-^*$, $\Phi_- \to \Phi_+^*$, where the asterisk stands for the complex conjugate. On the other hand, the self-repulsion makes the effective mass of the gap soliton negative, hence one may expect that the trapping potential

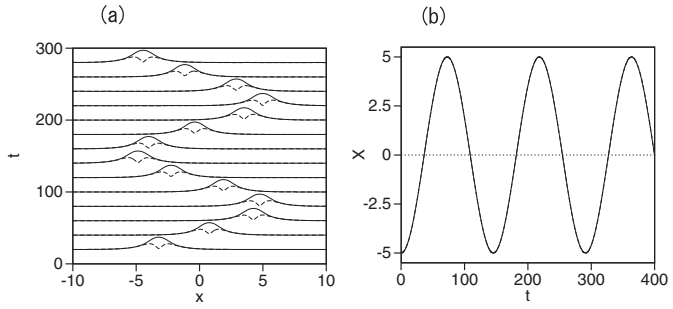

FIG. 2: (a) Continuous and dashed lines depict the evolution of $|\Phi_+|$ and $|\Phi_-|$ for a 1D gap soliton which performs harmonic oscillations in the trapping potential with $k = 0.0025$, $\Omega = 1$, $g = 1$, and $\gamma = 0$ in Eq. (23). (b) The respective evolution of the soliton's central coordinate, $X(t)$.

will become expulsive for it [46, 47]. Here, we address this point by simulating the 1D system in the form of

$$\begin{aligned} i\frac{\partial \Phi_+}{\partial t} &= \frac{\partial \Phi_-}{\partial x} + (\tilde{g}|\Phi_+|^2 + \tilde{\gamma}|\Phi_-|^2)\Phi_+ + \frac{1}{2}kx^2\Phi_+ + \Omega\Phi_+, \\ i\frac{\partial \Phi_-}{\partial t} &= -\frac{\partial \Phi_+}{\partial x} + (\tilde{g}|\Phi_-|^2 + \tilde{\gamma}|\Phi_+|^2)\Phi_- + \frac{1}{2}kx^2\Phi_- - \Omega\Phi_-, \end{aligned} \tag{26}$$

with $\tilde{g} = 1$, $\tilde{\gamma} \geq 0$ and $k > 0$, which implies the interplay of the repulsive nonlinearity and normal trapping potential.

As expected, the simulations demonstrate, in Fig. 3, that the gap soliton is expelled by the trapping potential: starting from the initial position, $X(t = 0)$, the soliton moves with $X(t) = 0.1\cosh(\lambda t)$ with $\lambda = 0.00877$. Comparing this with the equation of motion for a particle in potential $(1/2)kx^2$, we conclude that its effective mass is $m_{\rm eff} = -k/\lambda^2 \approx -1.30$, cf. the positive effective mass (25) of the gap soliton in the case of the attractive nonlinearity.

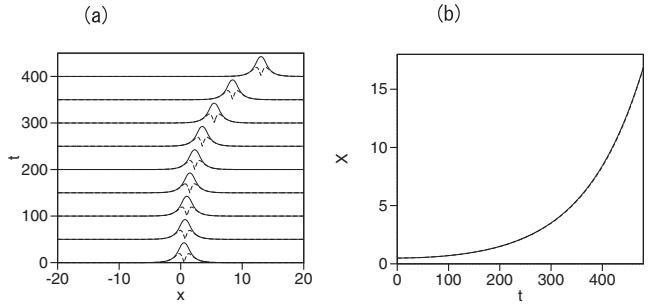

FIG. 3: The same as in Fig. (2), but in the case of the interplay of the self-repulsive nonlinearity and trapping potential, as per Eq. (26) with $k = 0.0001$, $\Omega = -1, \tilde{g} = 1$, and $\tilde{\gamma} = 0$.

D. An exact solution for the linear system

To complete the discussion of the 1D system placed in the trapping potential, we note that it admits an exact solution in the linear limit, $g = \gamma = 0$, if the Zeeman splitting is absent too, $\Omega = 0$. Indeed, in this case the solution of Eq. (23) is easily found as

$$\begin{aligned} \Phi_+(x,t) &= \frac{1}{2}\left[\exp\left(\frac{i}{6}kx^3\right)\phi_1^{(\rm arb)}(x+t) + \exp\left(-\frac{i}{6}kx^3\right)\phi_2^{(\rm arb)}(x-t)\right], \\ \Phi_-(x,t) &= \frac{i}{2}\left[\exp\left(\frac{i}{6}kx^3\right)\phi_1^{(\rm arb)}(x+t) - \exp\left(-\frac{i}{6}kx^3\right)\phi_2^{(\rm arb)}(x-t)\right], \end{aligned} \tag{27}$$

where $\phi_{1,2}^{(\mathrm{arb})}(x \pm t)$ are arbitrary complex functions of their arguments, which are determined if initial conditions, $\Phi_{\pm}(x, t=0)$, are specified:

$$\phi_1^{(\mathrm{arb})}(x) = \exp\left(-\frac{i}{6}kx^3\right)\left[\Phi_+(x,t=0) - i\Phi_-(x,t=0)\right],$$
$$\phi_2^{(\mathrm{arb})}(x) = \exp\left(\frac{i}{6}kx^3\right)\left[\Phi_+(x,t=0) + i\Phi_-(x,t=0)\right]. \tag{28}$$

In particular, the numerical solution of Eq. (23) with $g = \gamma = \Omega = 0$ and $k = 0.125$, generated by initial conditions

$$\Phi_+(x, t=0) = \Phi_-(x, t=0) = \exp\left(-x^2\right), \tag{29}$$

displayed in Fig. 4, exactly corresponds to the analytical solution given by equations (27) and (28). That is, the Gaussian input splits into two wavelets traveling with speeds ± 1, whose motion is not affected by the trapping potential.

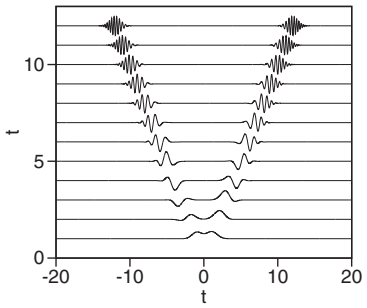

FIG. 4: Time evolution of $\mathrm{Re}\,(\Phi_+)$, as obtained from numerical solution of Eq. (23) with $g = \gamma = \Omega = 0$, $k = 0.125$, and initial conditions (29). It is identical to the analytical solution given by Eqs. (27)-(29).

IV. TWO-DIMENSIONAL GAP SOLITONS IN THE FREE SPACE

In terms of polar coordinates (r, θ), soliton solutions to the 2D system (3) can be looked for in the form of the semi-vortex ansatz, which has the same general form as in Refs. [10] and [13] (where, unlike the present analysis, the GPE system included the kinetic-energy terms):

$$\Phi_+(r,\theta,t) = e^{-i\mu t}\phi_+(r),\ \Phi_-(r,\theta,t) = e^{-\mu t}e^{i\theta}\phi_-(r). \tag{30}$$

The substitution of this ansatz in Eq. (3) leads to the system of radial equations for real amplitudes $\phi_{\pm}$:

$$\frac{d\phi_-}{dr} = \mu\phi_+ - \frac{\phi_-}{r} - \Omega\phi_+ + (g\phi_+^2 + \gamma\phi_-^2)\phi_+, \tag{31}$$
$$\frac{d\phi_+}{dr} = -\mu\phi_- - \Omega\phi_- - (g\phi_-^2 + \gamma\phi_+^2)\phi_-. \tag{32}$$

Localized solutions to Eqs. (31), (32) can be readily obtained by means of the shooting method. Here, we use scaling to fix $g = \Omega = 1$. The family of semi-vortex solitons is characterized by the dependence of μ on the 2D norm,

$$N = 2\pi\int_0^\infty (|\phi_+|^2 + |\phi_-|^2) r dr, \tag{33}$$

which is displayed in Fig. 5(a) in the absence of the cross-nonlinearity, $\gamma = 0$.

The branch of the semi-vortex family with $d\mu/dN < 0$ in Fig. 5(a) is expected to be stable, while the other one, with $d\mu/dN > 0$, should be definitely unstable, according to the VK criterion. To check this expectation, we have performed systematic simulations of the perturbed evolution in the framework of Eq. (3). The simulations were run in the 2D domain of extension 30×30 in the present scaled units, using the mesh size 256×256 and the Runge-Kutta algorithm for marching forward in time.

Results of the simulations completely corroborate the stability of the branch which meets the VK criterion, even if, strictly speaking, it does not produce a sufficient stability condition. As a typical example, Fig. 5(b) demonstrates the evolution of $|\Phi_+|$ and $|\Phi_-|$ for $N = 7.075$ and $\mu = 0.796$, which is a semi-vortex soliton with amplitude $\phi_+(r = 0) = 1$, see Eq. (30). On the other hand, Fig. 5(c) confirms the instability of the soliton with $N = 8.443$, $\mu = 0.2672$, and $\phi_+(r = 0) = 2.1$, which belongs to the lower branch in 5(a), with the positive slope, $d\mu/dN > 0$. This unstable soliton (as well as others belonging to the same branch) eventually suffers blowup (collapse), which is a typical outcome of the evolution of unstable 2D solitons in systems with the cubic self-attraction [36].

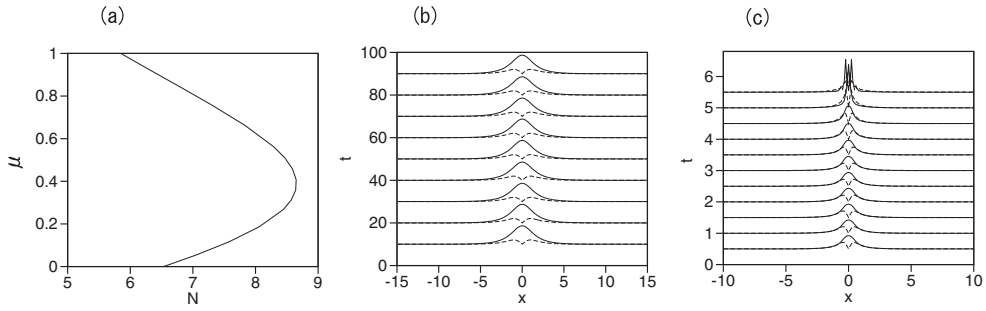

FIG. 5: (a) Chemical potential μ vs. norm N of the family of the 2D gap solitons based on the semi-vortex ansatz (30), as obtained from the numerical solution of Eqs. (31) and (32) with $g = \Omega = 1$ and $\gamma = 0$. Here and in Fig. 6(a) below, curves $\mu(N)$ are not shown for $-1 < \mu < 0$, as in that interval they represent definitely unstable solitons, which do not satisfy the Vakhitov-Kolokolov criterion, $d\mu/dN < 0$. (b) Stable evolution of components $|\Phi_+(x, y)|$ and $|\Phi_-(x, y)|$ (solid and dashed lines, respectively) of the 2D soliton with $\mu = 0.796$, shown in cross section $y = 0$. (c) The same as in (b), but for an unstable 2D soliton with $\mu = 0.2672$.

As shown in Refs. [10], [13], and [49], the interplay of the nonlinear cross- and self-interactions in the 2D SO-coupled system has a strong effect of the existence and stability of solitons. To address this point, in Fig. 6(a) we display a set of $\mu(N)$ curves for families of gap semi-vortex solitons with fixed $g = \Omega = 1$ (as mentioned above) and different relative strengths of the cross-interaction, $\gamma = 1$, 0.5, 0, and -0.5 (recall that $\gamma < 0$ corresponding to the repulsive sign of the cross interaction). For the sake of completeness, the set includes, as a particular case, the curve for $\gamma = 0$ from Fig. 5(a). An important fact is that VK-stable segments, with $d\mu/dN < 0$, do not exist at

$$\gamma > \gamma_{\max} \approx 0.77, \tag{34}$$

hence all the 2D gap solitons are *completely unstable* in this case. This conclusion agrees with the result reported in Ref. [19], where it was found that all the 2D gap solitons in the system with the local interactions are unstable for $\gamma = 1$.

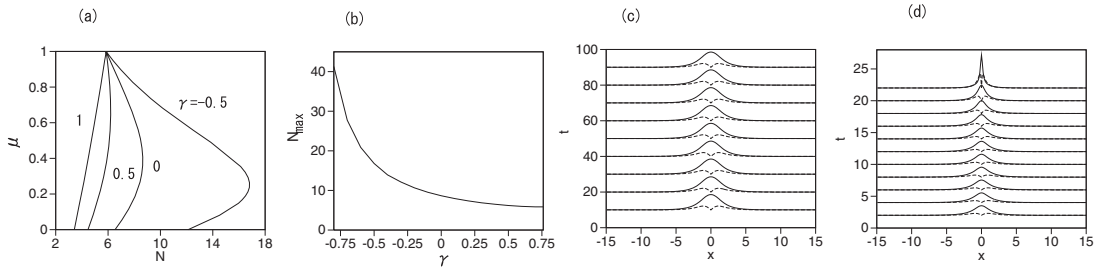

FIG. 6: (a) Curves $\mu(N)$ for families of 2D gap solitons of the semi-vortex type for $g = \Omega = 1$ and different values of the relative strength of the cubic interaction between the two components of the spinor wave function: $\gamma = 1$, 0.5, 0, and -0.5. Note that VK-stable segments of the $\mu(N)$ curves, with the negative slope, do not exist at $\gamma > \gamma_{\max}$, see Eq. (34). (b) The largest values of the norm from the curves in panel (a), $N_{\max}$, vs. γ. (c) The evolution of $|\Phi_+(x, y)|$ and $|\Phi_-(x, y)|$ (solid and dashed lines, respectively), shown in cross section $y = 0$, for a stable gap soliton, with $\mu = 0.784$, at $\gamma = -0.5$. (d) The same, but for an unstable soliton, with $\mu = 0.8135$, at $\gamma = 1$.

Thus, each $\mu(N)$ curve, plotted for $\gamma < \gamma_{\max}$, features point $N_{\max}$ which is the boundary between the VK-stable and unstable branches, with $d\mu/dN < 0$ and $d\mu/dN > 0$, respectively. The dependence of $N_{\max}$ on γ is displayed in

Fig. 6(b). It is worthy to note that $N_{\max}$ increases indefinitely at $\gamma \to -1$. This property is explained by the fact that, at $\gamma = -1$, the self-attractive and cross-repulsive interactions with equal strengths ($g = -\gamma = 1$) may nearly cancel each other, thus helping to create gap solitons at arbitrarily large N.

Another feature revealed by Fig. 6(a) is that all the $\mu(N)$ curves originate, at $\mu = 1$, from a single point, with the norm corresponding to the Townes' soliton, which is the fundamental solution of the single 2D GPE with the cubic self-attraction and normal kinetic-energy term [36]: $N = N_{\rm Townes} \approx 5.85$. The same is the smallest value of $N_{\max}$ attained at $\gamma \to \gamma_{\max}$, as can be seen in Fig. 6(b). This feature can be explained by noting that, close to the top edge of the bandgap, i.e., at $\mu \to 1$ (recall we are using normalization $\Omega = 1$), Eq. (32) yields a small component ϕ_-, which may be approximately eliminated in favor of the larger one (cf. a similar approach developed, in a different context, in Ref. [13]): $\phi_- \approx -(1/2)\, d\phi_+/dr$. Substituting this in Eq. (32), we arrive at the single GPE in which the effective kinetic-energy term is effectively restored:

$$(\mu - 1)\phi_+ = -\frac{1}{2}\left(\frac{d^2}{dr^2} + \frac{1}{r}\frac{d}{dr}\right)\phi_+ - \phi_+^3. \tag{35}$$

It is well known that Eq. (35) generates a family of 2D Townes' solitons, all having the same value of the norm, $N = N_{\rm Townes}$, which explains that all the branches originate from this value of N in Fig. 6(a).

Lastly, Figs. 6(c) and (d) illustrate, severally, the stability and instability of the gap solitons at $\gamma \neq 0$ [cf. the examples shown for $\gamma = 0$ in Figs. 5(b) and (b), respectively]: the stable soliton is produced with $N = 7.075$, $\mu = 0.784$, and amplitude $\phi_+(r = 0) = 1$ for $\gamma = -0.5$, while the unstable one, which eventually blows up, is obtained with $N = 5.45$, $\mu = 0.8135$, and the same amplitude, $\phi_+(r = 0) = 1$, at $\gamma = 1$.

The semi-vortices based on ansatz (30) represent fundamental gap solitons. Following Ref. [10], it is possible to introduce a more general ansatz, also compatible with system (3) of the SO-coupled GPEs, for *excited states* of the solitons, which are obtained by adding common integer vorticity m to both components of the spinor wave function:

$$\Phi_+ = e^{-i\mu t} e^{im\theta} \phi_+^{(m)},\ \Phi_- = e^{-\mu t} e^{i(m+1)\theta} \phi_-^{(m)}(r), \tag{36}$$

with real functions $\phi_\pm^{(m)}$ satisfying a system of radial equations:

$$\frac{d\phi_-^{(m)}}{dr} = \mu\phi_+^{(m)} - \frac{m\phi_-^{(m)}}{r} - \Omega\phi_+^{(m)} + \left[g\left(\phi_+^{(m)}\right)^2 + \gamma\left(\phi_-^{(m)}\right)^2\right]\phi_+^{(m)}, \tag{37}$$

$$\frac{d\phi_+^{(m)}}{dr} = -\mu\phi_-^{(m)} + \frac{(m+1)\phi_+^{(m)}}{r} - \Omega\phi_-^{(m)} - \left[g\left(\phi_-^{(m)}\right)^2 + \gamma\left(\phi_+^{(m)}\right)^2\right]\phi_-^{(m)}, \tag{38}$$

cf. Eqs. (30) and (31), (32). Localized solutions to Eqs. (37) and (38) can be again obtained with the help of the shooting method. Figure 7(a) displays the $\mu(N)$ curve for the family of the excited states with $m = 1$ and $\gamma = 0$.

However, unlike the fundamental semi-vortex solitons, all the excited states are found to be unstable in direct simulations, although their $\mu(N)$ curve still demonstrates, in Fig. 7(a), a segment satisfying the VK criterion (this fact stresses that the criterion is a necessary but not sufficient stability condition). A typical example of the instability onset is displayed in Fig. 7(b) for an excited state with $m = 1$, $N = 31.25$, $\mu = 0.66$, whose stationary form is characterized by slope $d\phi_+/dr = 0.6$ at $r = 0$. The instability spontaneously breaks the soliton's symmetry and eventually leads to the collapse. Note that all the excited states of semi-vortex solitons were also found to be unstable in the system considered in Ref. [10], which included the kinetic-energy terms and did not include the Zeeman splitting.

V. CONCLUSION

In this work we have demonstrated a novel mechanism for the formation of stable 2D and 1D solitons in the free space, built by the SO (spin-orbit) coupling combined with the sufficiently strong Zeeman splitting. While we consider the SO coupling of the Rashba type, it is natural to expect that more general forms of the coupling, such a Rashba-Dresselhaus [50] mixture, will produce similar results, cf. Ref. [13], which analyzed such a situation for ordinary solitons in the 2D system including the kinetic-energy terms. Following recent work [19], we consider the limit case when the energy of the SO coupling in the 2D system is much larger than the kinetic energy, making it possible to neglect terms accounting for the latter in the system of coupled GPEs (Gross-Pitaevskii equations). In the combination with the Zeeman splitting, the system changes its linear spectrum, opening a finite bandgap in it. In Ref. [19], it was recently demonstrated that, in the case of equal strengths of the self- and cross interactions between two components of the spinor wave function, the cubic contact nonlinearity fails to produce stable 2D gap

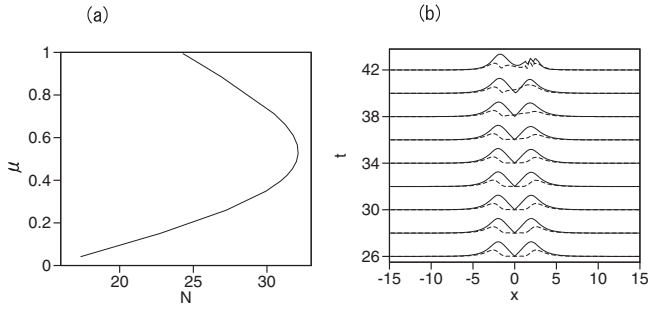

FIG. 7: (a) The $\mu(N)$ curve for the family of excited states, based on Eq. (36), with $g = \Omega = 1$, $\gamma = 0$, and $m = 1$. (b) Unstable evolution of $|\Phi_+(x, y)|$ and $|\Phi_-(x, y)|$ (solid and dashed lines, respectively), shown in cross section $y = 0$, of a typical excited state with $m = 1$.

solitons in the bandgap, therefore the analysis presented in Ref. [19] relied upon the use of long-range dipole-dipole interactions. The main finding reported here is that the contact interactions of either sign, attractive or repulsive, create *stable* 2D fundamental gap solitons of the semi-vortex type (with vorticities 0 and 1 in the two components), provided that the strength of the cross interaction, normalized to that of the self-interaction, does not exceed the critical value, ≈ 0.77. The boundary between stable and unstable subfamilies of 2D gap solitons in the bandgap is exactly predicted by the VK (Vakhitov-Kolokolov) criterion. Excited states of the semi-vortex solitons, created by adding equal vorticities to each component, are found too in the bandgap, but they are completely unstable. The analysis has also been performed for the 1D reduction of the system. In that case, the family of fundamental gap solitons, completely filling the bandgap, was found in the exact analytical form, the entire family being stable. In the 1D system, motion of the gap soliton in the trapping potential was studied too. The sign of the soliton's effective mass is positive or negative, respectively, in the case of the attractive or repulsive sign of the cubic nonlinearity. In particular, the trapping potential was shown to be expulsive for the gap solitons with the negative dynamical mass.

This work may be extended by considering moving 2D and 1D solitons and collisions between them, as suggested by Eqs. (7) and (9). In particular, it is interesting to find out how the motion affects the stability of the 2D gap solitons.

Acknowledgments

The work of B.A.M. is supported, in part, by the joint program in physics between NSF and Binational (US-Israel) Science Foundation through project No. 2015616, and by the Israel Science Foundation, through grant No. 1287/17.

[1] Y.-J. Lin, K. Jiménez-García, I. B. Spielman, Nature (London), **471**, 83 (2011).
[2] D. L. Campbell, G. Juzeliūnas, and I. B. Spielman, Phys. Rev. A **84**, 025602 (2011); Y. Zhang, L. Mao, and C. Zhang, Phys. Rev. Lett. **108**, 035302 (2012).
[3] Z. Wu, L. Zhang, W. Sun, X.-T. Xu, B.-Z. Wang, S.-C. Ji, Y. Deng, S. Chen, X.-J. Liu, and J.-W. Pan, Science **354**,83 (2016).
[4] V. Galitski and I. B. Spielman, Nature **494**, 49 (2013); H. Zhai, Rep. Progr. Phys. **78**, 026001 (2015).
[5] T. Kawakami, T. Mizushima, and K. Machida, Phys. Rev. A 84, 011607 (2011); H. Sakaguchi and B. Li, Phys. Rev. A 87, 015602 (2013).
[6] G. J. Conduit, Phys. Rev. A **86**, 021605(R) (2012).
[7] C. J. Wu, I. Mondragon-Shem, and X.-F. Zhou, Chin. Phys. Lett. **28**, 097102 (2011); T. Kawakami, T. Mizushima, M. Nitta, and K. Machida, Phys. Rev. Lett. 109, 015301 (2012).
[8] Y. Xu, Y. Zhang, and B. Wu, Phys. Rev. A **87**, 013614 (2013); V. Achilleos, D. J. Frantzeskakis, P. G. Kevrekidis, and D. E. Pelinovsky, Phys. Rev. Lett. **110**, 264101 (2013); Y. V. Kartashov, V. V. Konotop, and F. Kh. Abdullaev, *ibid.* **111**, 060402 (2013); L. Salasnich and B. A. Malomed, Phys. Rev. A **87**, 063625 (2013); L. Wen, Q. Sun, Y. Chen, D.-S. Wang, J. Hu, H. Chen, W.-M. Liu, G. Juzeliūnas, B. A. Malomed, and A.-C. Ji, Phys. Rev. A **94**, 061602(R) (2016); Y. V. Kartashov and V. V. Konotop, Phys. Rev. Lett. **118**, 190401 (2017).
[9] O. Fialko, J. Brand, and U. Zülicke, Phys. Rev. A **85**, 051605(R) (2012).
[10] H. Sakaguchi, B. Li, and B. A. Malomed, Phys. Rev. E **89**, 032920 (2014).

[11] V. E. Lobanov, Y. V. Kartashov, and V. V. Konotop, Phys. Rev. Lett. **112**, 180403 (2014); L. Salasnich, W. B. Cardoso, and B. A. Malomed, Phys. Rev. A **90**, 033629 (2014).
[12] Y.-C. Zhang, Z.-W. Zhou, B. A. Malomed, and H. Pu, Phys. Rev. Lett. **115**, 253902 (2015).
[13] H. Sakaguchi, E. Y. Sherman, and B. A. Malomed, Phys. Rev. E **94**, 032202 (2016).
[14] B. A. Malomed, D. Mihalache, F. Wise, and L. Torner, J. Optics B: Quant. Semicl. Opt. **7**, R53 (2005); B. A. Malomed, D. Mihalache, F. Wise, and L. Torner, J. Phys. B: At. Mol. Opt. Phys. **49**, 170502 (2016).
[15] D. Mihalache, Rom. J. Phys. **57**, 352 (2012)
[16] B. A. Malomed, Eur. Phys. J. Special Topics **225**, 2507-2532 (2016).
[17] S. Sinha, R. Nath, and L. Santos, Phys. Rev. Lett. **107**, 270401 (2011).
[18] B. Ramachandhran, B. Opanchuk, X.-J. Liu, H. Pu, P. D. Drummond, and H. Hu, Phys. Rev. A **85**, 023606 (2012).
[19] Y. Li, Y. Liu, Z. Fan., W. Pang, S. Fu, and B. A. Malomed, Phys. Rev. A **95**, 063613 (2017).
[20] Y. A. Bychkov and E. I. Rashba, J. Phys. C **17**, 6039 (1984); E. I. Rashba and E. Y. Sherman, Phys. Lett. A **129**, 175 (1988).
[21] D. L. Campbell, G. Juzeliūnas, and I. B. Spielman, Phys. Rev. A **84**, 025602 (2011).
[22] A. B. Aceves and S. Wabnitz, Phys. Lett. A **141**, 37 (1989); D. N. Christodoulides and R. I. Joseph, Phys. Rev. Lett. **62**, 1746 (1989); C. M. de Sterke and J. E. Sipe, **33**, 203 (1994).
[23] B. J. Eggleton, R. E. Slusher, C. M. de Sterke, P. A. Krug, and J. E. Sipe, Phys. Rev. Lett. **76**, 1627-1630 (1996).
[24] E. A. Ostrovskaya, J. Abdullaev, M. D. Fraser, A. S. Desyatnikov, and Yu. S. Kivshar, Phys. Rev. Lett. **110**, 170407 (2013); E. A. Cerda-Méndez, D. Sarkar, D. N. Krizhanovskii, S. S. Gavrilov, K. Biermann, M. S. Skolnick, and P. V. Santos, *ibid.* **111**, 146401 (2013).
[25] V. A. Brazhnyi and V. V. Konotop, Mod. Phys. Lett. B **18**, 627 (1994); O.Morsch and M. Oberthaler, Rev. Mod. Phys. **78**, 179 (2006).
[26] B. Eiermann, T. Anker, M. Albiez, M. Taglieber, P. Treutlein, K. P. Marzlin, and M. K. Oberthaler, Phys. Rev. Lett. **92**, 230401 (2004).
[27] H.-Y. Hui, Y. Zhang, C. Zhang, and V. W. Scarola, Phys. Rev. A **95**, 033603 (2017).
[28] T.-L. Ho, Phys. Rev. Lett. **81**, 742 (1998).
[29] Y. Deng, J. Cheng, H. Jing, C.-P. Sun, and S. Yi, Phys. Rev. Lett. **108**, 125301 (2012).
[30] R. M. Wilson, B. M. Anderson, and C. W. Clark, Phys. Rev. Lett. **111**, 185303 (2013); S. C. Ji, L. Zhang, X. T. Xu, Z. Wu, Y. J. Deng, S. Chen, and J. W. Pan, *ibid.* **114**, 105301 (2015); Y. Xu, Y. Zhang, and C. Zhang, Phys. Rev. A **92**, 013633 (2015); X. Jiang, Z. Fan, Z. Chen, W. Pang, Y. Li, and B. A. Malomed, *ibid.* **93**, 023633 (2016); T. Oshima and Y. Kawaguchi, *ibid.* **93**, 053605 (2016).
[31] I. Tikhonenkov, B. A. Malomed, and A. Vardi, Phys. Rev. Lett. **100**, 090406 (2008); P. Köberle, D. Zajec, G. Wunner, and B. A. Malomed, Phys. Rev. A **85**, 023630 (2012).
[32] J. Yang, B. A. Malomed, and D. J. Kaup, Phys. Rev. Lett. **83**, 1958 (1999); A. R. Champneys, B. A. Malomed, J. Yang, and D. J. Kaup, Physica D 152, 340-354 (2001); J. Yang, Phys. Rev. A **82**, 053828 (2010).
[33] S. B. Papp, J. M. Pino, and C. E. Wieman, Phys. Rev. Lett. **101**, 040402 (2008); P. Zhang, P. Naidon, and M. Ueda, *ibid.* **103**, 133202 (2009); F. Wang, X. Li, D. Xiong, and D. Wang, J. Phys. B: At. Mol. Opt. Phys. **49**, 015302 (2016).
[34] S. Giovanazzi, A. Görlitz, and T. Pfau, Phys. Rev. Lett. **89**, 130401 (2002).
[35] M. Vakhitov and A. Kolokolov, Quantum Electron. **16**, 783 (1973).
[36] L. Bergé, Phys. Rep. **303**, 259 (1998); G. Fibich, *The Nonlinear Schrödinger Equation: Singular Solutions and Optical Collapse* (Springer: Cham, 2015).
[37] V. Gurarie and J. T. Chalker, Phys. Rev. B **68**, 134207 (2003).
[38] O. Vafek and A. Vishwanath, Ann. Rev. Cond. Matt. **5**, 83-112 (2014).
[39] L. H. Haddad and L. D. Carr, Physica D, **238**, 1413 (2009); L. H. Haddad,C. M. Weaver, and L. D. Carr, New J. Phys. 17, 063033 (2015); L. H. Haddad and L. D. Carr, New J. Phys. **17** 063034 (2015); M. J. Ablowitz, and Y. Zhu, SIAM J. Appl. Math. **72**, 240 (2012).
[40] D. E. Pelinovsky and A. Stefanov, J. Math. Phys. **53**, 073705 (2012); L. H. Haddad and L. D. Carr, New J. Phys. **17**, 113011 (2015).
[41] J. Cuevas-Maraver, P. G. Kevrekidis, A. Saxena, A. Comech, and R. Lan, Phys. Rev. Lett. **116**, 214101 (2016).
[42] L. Salasnich, A. Parola, and L. Reatto, Phys. Rev. A **65**, 043614 (2002).
[43] A. Muryshev, G. V. Shlyapnikov, W. Ertmer, K. Sengstock, and M. Lewenstein, Phys. Rev. Lett. **89**, 110401 (2002).
[44] L. Salasnich and B. A. Malomed, Phys. Rev. A **74**, 053610 (2006).
[45] H. Sakaguchi and B. A. Malomed, New J. Phys. **18**, 105005 (2016).
[46] H. Sakaguchi and B. A. Malomed. J. Phys. B **37**, 1443 (2004).
[47] M. Salerno, V. V. Konotop, and Yu. V. Bludov, Phys. Rev. Lett. **101**, 030405 (2008).
[48] O. Zobay, S. Potting, P. Meystre, and E. M. Wright, Phys. Rev. A **59**, 643 (1999); P. J. Y. Louis, E. A. Ostrovskaya, C. M. Savage, and Y. S. Kivshar, *ibid.* **67**, 013602 (2003); N. K. Efremidis and D. N. Christodoulides, *ibid.* **67**, 063608 (2003).
[49] Y. Li, Z. Luo, Y. Liu, Z. Chen, C. Huang, S. Fu, H. Tan, and B. A. Malomed, New J. Phys., in press.
[50] G. Dresselhaus, Phys. Rev. **100**, 580 (1955).